ELSEVIER

Journal of Nuclear Materials 277 (2000) 211–216

journal of nuclear materials

www.elsevier.nl/locate/jnucmat

Effects of the porosity in uranium dioxide on microacoustic and elastic properties

V. Roque[a], B. Cros[a,*], D. Baron[b], P. Dehaudt[c]

[a] *LAIN, Université Montpellier 2, 34095 Montpellier cedex 05, France*

[b] *EDF, Division Recherches et Développements, 77250 Moret/Loing, France*

[c] *Commissariat à l'Energie Atomique, Département d'Etudes des Combustibles, 17 avenue des Martyrs, 38054 Grenoble cedex 09, France*

Received 20 May 1999; accepted 21 July 1999

Abstract

The laws of variation of the Rayleigh velocity and the longitudinal velocity of the acoustic waves as a function of the porosity in uranium oxide UO_2 has been proven through local acoustic measurements carried out, respectively, by acoustic microscopy and by microechography. The variations of the elastic constants with porosity have been deduced from these laws. Thanks to these results, the role of porosity can be separated and the part of the other factors in the alteration of elastic properties of nuclear fuel materials can be highlighted. These new investigation methods, combined with microindentation techniques are expected to be helpful in improving the nuclear fuel material characterisation at high burn-up.

PACS: 6200; 8170B; 2846; 2842

1. Introduction

The fuel materials used in pressurised water reactors are designed in the shape of uranium dioxide pellets mixed or not with plutonium dioxide, 8 mm in diameter, piled on 3.6 m in a Zircaloy tubing, 4 m long, closed at its ends by two sealed Zircaloy plugs and pressurised with helium. The integrity of the Zircaloy cladding must be warranted at every time of the life of the so-called 'fuel rod'. In order to evaluate the mechanical interaction between the fuel stack and the tubing, code simulations are used by the designers. The simulation is done, assuming the effects of the pellets cracking pattern and accounting for the different phenomena involved during irradiation (densification, swelling, cladding creep down...). A good characterisation of the fuel material is required at each time of the irradiation to allow an accurate evaluation of the strain fields. These characterisations concern the local thermal or mechanical properties but also the parameters having a strong influence on these properties: porosity, cracking pattern, lattice damage...

At the present time, two complementary techniques, micro-indentation and microacoustic, are developed to characterise the mechanical behaviour of the irradiated fuel pellets. The effects of irradiation varying according to a radial gradient, localised characterisations are required. The 200 μm wide 'rim' region, in contact with the cladding and mostly modified by the irradiation (mainly due to the Uranium 238 self shielding effect and operating temperatures preventing from any recovering processes), justifies if necessary such localised measurements. Micro-indentation characterises plastic properties and, indirectly through modelling, elastic properties. Microacoustic characterises elastic properties. The aim of this work has been to demonstrate the capabilities of the acoustical techniques on irradiated and non-irradiated fuel ceramics. First, the effects of the fuel pellet porosity on their acoustical properties should be quantified in order that the intrinsic elastic properties can be deduced from measurements. Porosity calibrated

* Corresponding author. Tel.: +33-4 67 14 49 09; fax: +33-4 67 52 15 84.

E-mail address: cros@lain.univ-montp2.fr (B. Cros).

0022-3115/00/$ - see front matter
PII: S0022-3115(99)00192-0

samples have been manufactured using poreformers and different sintering conditions. Poreformers are currently used to control the density in order to limit the shrinkage at low burn-up and trap the gaseous fission products. This initial porosity then evolves during irradiation, according to the densification (irradiation induced sintering) and the vacancies coalescence.

2. Previous works

The dependence of the ultrasonic velocity on porosity has first been expressed in the form

$$V = V_0(1-p), \tag{1}$$

where V is the measured velocity, V_0 the velocity of the non-porous material and p the volume fraction of porosity. A better fit to the experimental data is obtained by the relation [1,2]

$$V = V_0(1-p)^{\alpha}. \tag{2}$$

The empirical constant α is related to a stress concentration factor around pores in the material and is dependent on pore geometry and its orientation in the material [3]. For porosities lower than 10%, the linear relation is used:

$$V = V_0(1-\alpha p). \tag{3}$$

The fit to experimental data on elastic modulus is provided by relations of the type

$$M = M_0 \exp(-\beta p) \tag{4}$$

and

$$M = M_0 \exp[-\beta p + \gamma p^2]. \tag{5}$$

M is the Young's modulus E or the shear modulus G, β and γ are empirical constants. The subscript 0 refers to the modulus of non-porous materials. According to physical acoustics theory, elastic moduli and ultrasonic velocities are related by

$$V_L = [E(1-v)/\rho(1+v)(1-2v)]^{1/2}, \tag{6}$$

and

$$V_S = (G/\rho)^{1/2}, \tag{7}$$

where V_L and V_S are longitudinal and transverse velocities respectively, v the Poisson's ratio and r is the density.

The study of the elastic constants alteration in uranium dioxide UO_2 as a function of the porosity rate has given rise to a wide number of works. Nevertheless, they are all supported by global measurements. We only refer to the synthesis of results published by Martin [4]. This author expresses the variation of elastic constants as a function of p by a linear relationship of type (4).

The most complete studies based on acoustic waves velocity measurements have been carried out by Panakkal. The works published in 1984 [5] fit the experimental data by a linear law with a correlation ratio of 0.99. The later works [6] do not so well agree with the experimental results because, on the one hand of the wide variety of experimental results, on the other of the extent of the porosity range investigated. In fact, the experimental studies available for other kinds of materials show that the variation of the acoustic waves velocity cannot be expressed by a linear law in a large scale of porosity. In the case of uranium dioxide, this scale should be limited to a volume fraction of porosity of 0.1. This corresponds to the range of porosity encountered in nuclear fuel materials.

In a previous work, we have presented the micro-acoustic techniques and their application on irradiated materials [7].

3. The materials

The samples provided are nuclear fuel pellets obtained by compression and sintering of a uranium dioxide powder, containing 0.2% of ^{235}U, with calibrated porosities volumes (Table 1). For each sample, the final porosity rate is established by hydrostatic weighing. The sample with lowest porosity ($p = 1.9\%$) has been prepared without poreformer, porosity volume being controlled only by sintering. The pores size is less than 2 μm. The highest porosities ($p = 2.75$–7.18%) have been obtained by adding poreformer and pore size distribution is centred both on 1 μm (about 1.7% of the porosity) and

Table 1
Microstructural features of the UO_2 samples (Average grain size $= (S/N)^{1/2}$)

Sample	1	2	3	4	5	6
Porosity $p\% \pm 0.01\%$	1.90	2.75	4.1	4.95	6.02	7.18
Average grain size[a] (μm ± 0.03 μm)	12.8	15.4	12.9	14.4	12.6	11.7
Average grain size[b] (μm ± 0.03 μm)	14.9	17.5	15.8	19.4	12.9	13.1

[a] Of the pellet.
[b] At the centre.

10 μm. All samples having the same stoichiometric composition $UO_{2,00}$ and the same microstructure (approximately same grain size), porosity is the only parameter whose role should be related to velocity alterations. A roughness around 1 μm is required for acoustic signature recording. It is carried out by polishing the upper face of the samples. Concerning the microechography measurements, the requirement is not so sharp, allowing a roughness around 5μm, but on the two faces of the 1 mm thick samples.

4. The microacoustic techniques

The acoustic microscopy technique and its advantages for the realisation of images and for the determination of local elastic properties on irradiated and non-irradiated uranium dioxide have been described earlier [7]. Local measurements are carried out through the acoustic signature or $V(z)$ of the material. This signature is processed by recording the reflected acoustic signal variation as a function of the defocus z of the sample surface moving from the focal plane towards the acoustic lens [8]. The $V(z)$ response can be quantified through the fast Fourier transform method. It gives the period of the pseudo-oscillations and then the velocities of different acoustic modes can be calculated from the formula [9]

$$V = V_f\left[1 - (1 - V_0/2f\Delta z)^2\right]^{-1/2}, \tag{8}$$

where V_f is the velocity in the coupling fluid, f is the operating frequency and Δz is the period of the pseudo-oscillations. The surface waves being very sensitive to the properties of the sample, the $V(z)$ response can give valuable information about local changes in the material constitution.

The porosity of UO_2 samples brings about diffusion. Increasing frequency, acoustic waves are more diffused and attenuated when the wavelength becomes of the same order as the pore dimensions. According to this phenomenon, porous uranium dioxide was revealed to be very absorbent at 580 MHz; acoustic signatures carried out at this frequency are not exploitable. Measurements have then been carried out successfully at 15 MHz and accurately reproducible. Elsewhere, the very high density of uranium oxide is unfavourable to the back-radiation of the acoustic waves towards the lens. This results in an insufficient efficiency of the various modes, especially the longitudinal mode. The only Rayleigh mode is involved in the acoustic signature and its velocity V_R can be accurately measured despite its low efficiency.

Then, in order to measure the longitudinal wave velocity, microechography [10] has been performed. Time position of the echoes corresponds to the distance covered by the longitudinal waves. All the experiments were carried out in transmission mode. Two sensors are set out in opposite, the one operating as emitter and the second as receiver. This device saves thickness measurements of the sample and the effects of possible lacks of parallelism between its faces are avoided. The transducer operates at a central frequency of 40 MHz chosen accounting for the 1 mm thickness of the samples. This frequency provides a pulse length sufficient to separate the echoes of the front face and the back face of the material. Echo 1, transmitted by sensor 1 and received by sensor 2 is first recorded. The sample is then placed on the beam path and echoes 2 and 3 are recorded. These measurements give the times of flight

$$\Delta t_1 = t_1 - t_2 \qquad \Delta t_2 = t_3 - t_2$$

from which the sample thickness d and the longitudinal velocity V_l in the sample are calculated by

$$d = V_0(\Delta t_1 + \Delta t_1/2), \tag{9}$$

$$V_l = V_0(2\Delta t_1/\Delta t_1 + 1). \tag{10}$$

V_0, the coupling fluid velocity, is measured apart. The choice of the coupling fluid should take into account the very high acoustical impedance of uranium dioxide, unfavourable to the penetration of acoustic waves in the sample. This can be verified by the relationship expressing the reflecting power R:

$$R = (Z_1 - Z_2)/(Z_1 + Z_2). \tag{11}$$

$Z = \rho V$ is the acoustical impedance, ρ the volume mass and V is the longitudinal velocity. Mediums 1 and 2 are, respectively, the uranium oxide sample and the coupling liquid.

The time position of each echo is obtained with an accuracy within ±0.1%, which gives an accuracy of about 1% on the values of the longitudinal velocity and the thickness.

The mechanical features, Young modulus E, shear modulus G and Poisson's coefficient v, as well as the Debye temperature Θ_D can be calculated from the measurement of V_L and V_T, the velocities of the longitudinal and transverse waves and from the knowledge of the density ρ:

$$E = \left[3 - 4(V_T/V_L)^2\right] \Big/ \left[1 - (V_T/V_L)^2\right] \rho V_T^2, \tag{12}$$

$$G = \rho V_T^2, \tag{13}$$

$$v = \left[2(V_T/V_L)^2 - 1\right] \Big/ 2\left[(V_T/V_L)^2 - 1\right] \rho V_T^2, \tag{14}$$

$\Theta_D = h \cdot v_D/k$ where h is the Planck constant, k the Boltzman constant, v_D being calculated from

$$v_D = \left[9N/4\pi a^3(1/V_L^3 + 2/V_T^3)\right]^{1/3},$$

where N is the number of atoms in a unit cell and a the lattice parameter of UO_2. The Debye temperature is an indication of the shape of the potential energy. Generally speaking, the Debye temperature in a compound increases with the average atomic mass or decrease in the inter-atomic distance. Nevertheless, the solid solution (U,Ce)O_2 formation, for instance, lowers the Debye temperature of UO_2, even though it yields the reduction in both the average mass and the atom distance [11].

The transverse velocity V_T is related to V_L and V_R by

$$4(V_T/V_R)^{1/2}\left(1-V_T^2/V_R^2\right)^{1/2}\left(V_T^2/V_L^2-V_T^2/V_R^2\right)^{1/2} + \left(1-2V_T^2/V_R^2\right)^{1/2} = (\rho_0/\rho_S)\left(V_T^2/V_L^2-V_T^2/V_R^2\right) / \left(V_T^2/V_0^2-V_T^2/V_R^2\right)^{1/2}. \quad (15)$$

In order to carry out local measurements, the acoustic microscope uses a focused sensor with an aperture angle of 50°. Microechography operates with a small diameter (1 mm) counter-electrode and a slightly focused beam (7°) to offset the beam divergence brought about by the diffraction of a small transmitting acoustic source. The result is a spot with a small diameter of about 500 μm.

5. Experimental results

Fig. 1 displays the values of the Rayleigh velocity V_R obtained by acoustic microscopy (through the acoustic signature). Each point represent an average of 20 measurements carried out in the same area. The variation of the Rayleigh velocity as a function of the porosity volume fraction p can be fitted by a linear relationship

$$V_R = 2565(1-0.67p). \quad (16)$$

Its validity should be limited to $p \leqslant 0.1$, which corresponds to the porosity currently met in the different nuclear fuel manufactured. Through measurements of the Rayleigh velocity, the porosity ratio in uranium

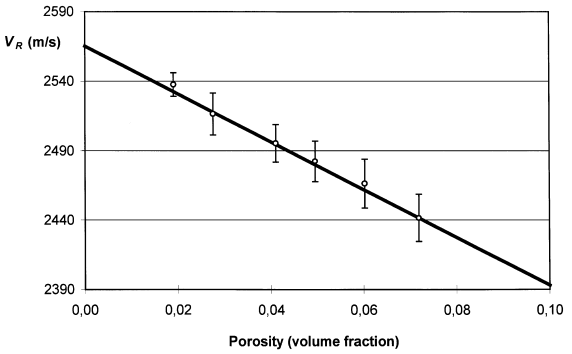

Fig. 1. Variation of the Rayleigh velocity as a function of the porosity of uranium oxide. The straight line represents the law of evolution deduced from measurements.

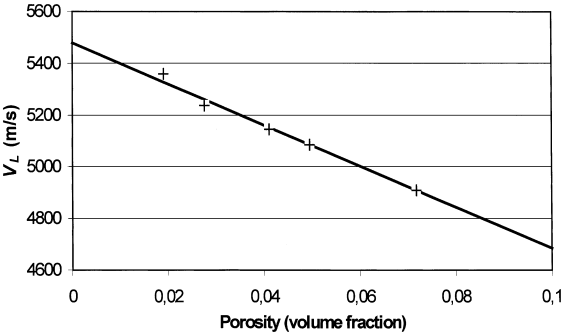

Fig. 2. Variation of the longitudinal velocity as a function of the porosity of uranium oxide. The points represent the experimental measurements. The straight line represents the law of evolution established by Panakkal [5].

oxide UO_2 can be determined thanks to this relationship with an accuracy of 0.5% if the error on V_R measurements is not higher as 10 m s^{-1}. The good agreement met with all the experimental data in Fig. 1, with the same law tends to show that V_R varies as a function of the porosity ratio and not as a function of the pore size, one sample having a porosity spectrum centred on 1 μm, the others on 10 μm.

Measurements of the longitudinal velocity V_L carried out by microechography in transmission (Fig. 2) agree with the previous works which express the variation of the longitudinal velocity as a function of porosity, for a ratio not higher as 10% by [5]

$$V_L = 5479(1-1.45p). \quad (17)$$

6. Discussion

This study shows that linear relationships exist between the porosity ratio in uranium oxide UO_2 and the acoustic waves velocities. Measurements have been limited to porosities ranging from 1.90% to 7.18%, which corresponds to the porosity of non-irradiated fuel. During irradiation, the porosity is modified, especially because of the fission activated resintering at the beginning of life, the swelling effect due to the fission gas and vacancies migration with the bubble coalescence and the creep phenomena at high temperature (combined with resintering). In particular, a bubble buildup is observed at local burn-up higher than 55 GWj/tU in the rim region; here the porosity can reach 10–12% for local burn-ups over 70 GWd/tM [12]; it is the more recent evaluation. A deviation from the linear law between acoustic velocity and porosity can be expected for high porosities. Fig. 3 displays the curves calculated by using the Berryman model to plot the variation of V_R for high porosities. This model has been established [13] to sim-

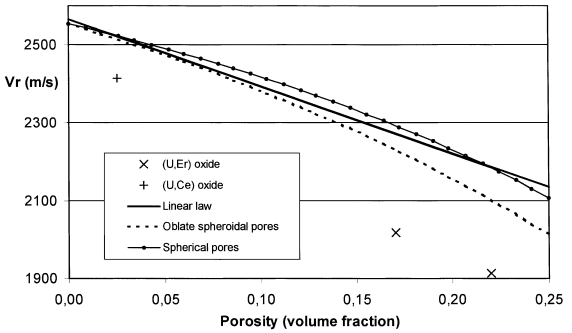

Fig. 3. Variation of the Rayleigh velocity in uranium dioxide UO_2 as a function of porosity calculated, from our results, according to: —— a linear law of evolution; - - - - - the Berryman model on the assumption of oblate spheroidal pores; ○ ○ ○○ the Berryman model on the assumption of spherical pores. The shift of velocity in $(U_{1-y}Ln_y)O_{2+x}$ solid solutions of lanthanoïd elements is marked by + for Ln = Ce and × for Ln = Er (the oxygen/metal ratio O/M = 2 + x of each phase is given close to the representative point).

ulate the alteration of the elastic properties of a material in the presence of micro-domains of a second phase. The corresponding curve fits with the experimental points on the assumption of oblate spheroidal pores with an aspect ratio $c/a = 0.4$. It shows a linear variation up to 10% porosity, then a bending toward lower velocities. The calculated curve considering spherical pores is given for comparison.

Concerning the laws of variation of elastic constants as a function of porosity they have been established (Figs. 4 and 5) through the relationships (16) and (17) using (12) and (13), giving

$$E = 220(1 - 2.34p), \tag{18}$$

$$G = 82(1 - 2.03p) \tag{19}$$

and can be compared to the laws established by Martin [4]:

$$E = 222(1 - 2.5p), \tag{20}$$

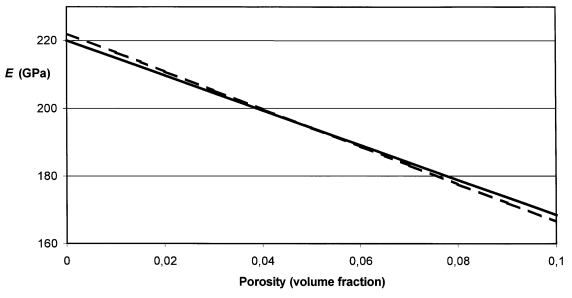

Fig. 4. Variation of Young's modulus as a function of the porosity of uranium oxide calculated through the acoustic wave velocity measurements. —— Our work; - - - - - Martin's work [4].

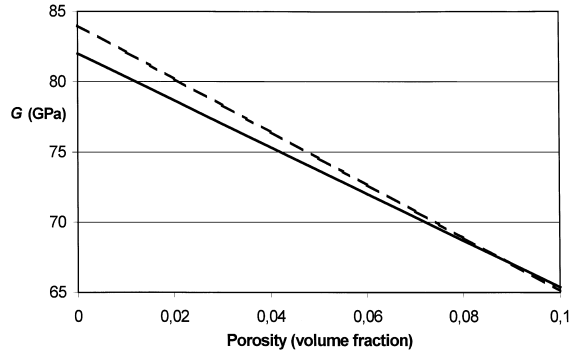

Fig. 5. Variation of shear modulus as a function of the porosity of uranium oxide calculated through the acoustic wave velocity measurements. —— Our work; - - - - - Martin's work [4].

$$G = 84(1 - 2.25p). \tag{21}$$

As a consequence, when the intrinsic Young's modulus of a material is known, the porosity ratio can be determined thanks to velocity measurement of the Rayleigh mode or/and the longitudinal mode. On the contrary, the porosity being known, velocity values corrected from the part of porosity can be calculated and used to have access to the knowledge of the intrinsic material Young's modulus.

However works are still under way to improve the method, because other parameters can obviously deteriorate the elastic properties of the irradiated UO_2:

- Any modification of the O/M (anion/cation) ratio involves a disturbance of the anionic sub-lattice likely to modify the velocity of acoustic waves and the Young's modulus [4,14,15] (at room temperature, according to the preparation conditions, non-irradiated UO_{2+x} often coexists in the presence of the higher oxides $U_4O_{9-\delta}$ and U_3O_{8-z} whose elastic properties are involved in measurements [14,16].
- The formation of solid solutions $(U_{1-y}Ln_y)O_{2+x}$ in the presence of lanthanoïds like cerium or gadolinium and erbium (neutrons absorbers) gives rise to alterations of the bond energies by formation, near to the U–O and U–U bonds, of Ln–O and U–Ln bonds with appreciably different energy. Analogous alterations take place through the formation of $(U,Pu)O_2$ with the plutonium fission product [17,18].
- Grain size [14] which decreases in the rim region and increases in the pellet heart.
- When the solubility limit of addition elements is exceeded, the appearance of secondary phases will also have an effect on the elastic properties.

In this way, measurements carried out on $(U_{1-y}Ln_y)O_{2+x}$ phases (Ln = Ce, Er) with known porosity (Fig. 3) show that the velocity values depart from the straight line as well as from the Berryman model which represents the part of porosity in V_R. This shift

yields the lowering of Young's modulus which goes with the alterations of the network when the solid solution is formed and previously a high O/M ratio.

7. Conclusion

The porosity measurements on irradiated fuel pellets, using optical or SEM image analysis are still controversial. There is then a need of an alternative method. This study establishes the relationship between porosity and elastic properties in a uranium dioxide UO_2. As a consequence, the part of porosity in the elastic properties can be corrected and the evolution of the intrinsic Young's modulus after additions in uranium oxide can be characterised.

The originalities of this work have been the development of combined techniques adapted for localised measurements limited to areas about some tenths of square millimetres. These allow accurate measurements of the longitudinal velocity and the Rayleigh velocity from which the local elastic properties and relative porosity volume can be deduced. These original techniques are potential methods for the characterisation of irradiated materials.

However, at this stage, the work performed at room temperature does not refer to the role of temperature on the elastic properties. This should be the aim of a separate study.

References

[1] K.K. Phani, S.K. Niyogi, J. Mater. Sci. Lett. 5 (1986) 427.
[2] K.K. Phani, S.K. Niyogi, A.K. Maitra, M. Roychaudhury, J. Mater. Sci. 21 (1986) 4335.
[3] A.K. Maitra, K.K. Phani, J. Mater. Sci. 29 (1994) 4415.
[4] D.G. Martin, High Temp.–High Press. 21 (1989) 13.
[5] J.P. Panakkal, J.K. Ghosh, J. Mater. Sci. Lett. 3 (1984) 835.
[6] J.P. Panakkal, IEEE Trans. Ferroelec. Freq. Control 38 (1991) 161.
[7] V. Roque, D. Baron, J. Bourgoin, J.M. Saurel, J. Nucl. Mater. 275 (1999) 305.
[8] R.J.M. da Fonseca, L. Ferdj-Allah, G. Despaux, A. Boudour, L. Robert, J. Attal, Adv. Mater. 5 (1993) 508.
[9] H. Bertoni, IEEE Trans. Sonics Ultrasonics SU-31 (1984) 105.
[10] R.J.M. da Fonseca, Y.M.B. de Almeida, B. Cros, J.M. Saurel, M.J.M. Abadie, Thin Solid Films 251 (1994) 110.
[11] K. Yamada, S. Yamanaka, T. Nakagawa, M. Uno, M. Katura, J. Nucl. Mater. 247 (1997) 289.
[12] J. Spino, D. Baron, M. Coquerelle, A.D. Stalios, J. Nucl. Mater. 256 (1998) 189.
[13] J.G. Berryman, J. Acoust. Soc. Am. 68 (1980) 1809.
[14] N. Igata, K. Domoto, J. Nucl. Mater. 45 (1972) 317.
[15] D.L. Hagrman, G.A. Raymann, R.E. Mason, US Nuclear Regulatory Comission Report NUREG/CR-0479, 1981.
[16] R.J. Forlano, A.W. Allen, R.J. Beals, J. Am. Ceram. Soc. 50 (1967) 93.
[17] A.W. Nutt, A.W. Allen, J.H. Handwerk, J. Am. Ceram. Soc. 53 (1970) 205.
[18] C. de Novion et al., Nucl. Metall. 17 (1970) 509.